PURPOSE-LED
PUBLISHING™

**PAPER**

# Electron impact excitation of the Tl⁺ ion: resonance and cascade transitions

To cite this article: Viktoria Roman *et al* 2022 *J. Phys. B: At. Mol. Opt. Phys.* **55** 165203

View the article online for updates and enhancements.

## You may also like

- Diagnostics of laser-produced Mg plasma through a detailed collisional radiative model with reliable electron impact fine structure excitation cross-sections and self-absorption intensity correction
  S S Baghel, S Gupta, R K Gangwar et al.

- Effect of anisotropic grain boundaries on the surface blistering of tungsten induced by deuterium plasma exposure
  Tongjun Xia, Zhenyu Jiang, Yongzhi Shi et al.

- Timing and energy stability of resonant dispersive wave emission in gas-filled hollow-core waveguides
  Christian Brahms and John C Travers

# Electron impact excitation of the Tl$^+$ ion: resonance and cascade transitions

**Viktoria Roman**[1], **Aleksandr I Gomonai**[1], **Lalita Sharma**[2],
**Aloka Kumar Sahoo**[2] **and Anna N Gomonai**[1,*]

[1] Institute of Electron Physics, Ukrainian National Academy of Sciences, Uzhhorod, 88017, Ukraine
[2] Indian Institute of Technology Roorkee, Roorkee, 247667, India

E-mail: annagomonai@gmail.com

## Abstract

Results of experimental and theoretical investigations into the electron-impact excitation of the resonance $6s6p\ ^1P_1^\circ \rightarrow 6s^2\ ^1S_0$ (132.2 nm), as well as the cascade $6s7s\ ^1S_0 \rightarrow 6s6p\ ^1P_1^\circ$ (309.2 nm) and $6p^2\ ^1D_2 \rightarrow 6s6p\ ^1P_1^\circ$ (150.8 nm) spectral transitions from the ground $6s^2\ ^1S_0$ level in the thallium ion, are presented. Crossed beams of electrons and Tl$^+$ ions in combination with a spectroscopic method were used in the experiment. Measured cross sections have a distinct resonance structure arising mainly from the electron decay of atomic $5d^96s^26p^2$, $5d^{10}6s7s(^1S)np$ ($n \geqslant 7$), $5d^{10}6s6d(^1D)np$ ($n \geqslant 6$), $5d^{10}6s6d(^1D)nd$ ($n \geqslant 6$) and ionic $5d^96s^2np$, $5d^96s^2nd$, $5d^96snp$ ($n \geqslant 6$) autoionizing levels, as well as radiative transitions from the higher $6s7s\ ^1S_0$, $6s6d\ ^1D_2$, and $6p^2\ ^1D_2$, $^1S_0$ ionic levels. Relativistic distorted wave (RDW) calculations are performed to obtain the effective cross sections for the above transitions. The absolute values of the cross sections are found to be $1.39 \times 10^{-16}$ cm$^2$ at 300 eV for the $\lambda$132.2 nm resonance line, and $0.11 \times 10^{-16}$ cm$^2$ and $0.56 \times 10^{-16}$ cm$^2$ at 100 eV for the $\lambda$309.2 nm and $\lambda$150.8 nm lines, respectively. The contribution of the cascade transitions being studied to the effective cross section of the $\lambda$132.2 nm resonance line at the energy of 100 eV is about 30%. A calculation using the semi-empirical Van Regemorter formula is also performed to obtain the effective cross section of the resonance $\lambda$132.2 nm line. The absolute value of the cross section at 300 eV is found to be nearly the same as that given by the RDW calculation.

(Some figures may appear in colour only in the online journal)

## 1. Introduction

The excitation of positive ions by electron impact plays a significant and sometimes dominant role in various types of laboratory and astrophysical plasmas. Therefore, understanding this process is of considerable interest for solving many problems in modern physics and for various applications. Plasma diagnostics using a beam of heavy ions such as Tl$^+$, so-called heavy ion beam probe diagnostics, is the only way to measure the electric potential in the hot region of plasma in toroidal thermonuclear facili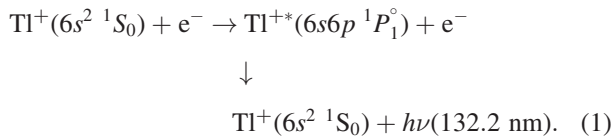ties [1]. Most emission lines observed in astrophysical studies result from the excitation of ions due to collision with electrons. In particular, Tl$^+$ ion spectral lines were identified in astrophysical observations of the Hg–Mn stars [2, 3]. Hence, a study of this process is vital for interpreting the spectra of the Sun and the stars. From the viewpoint of fundamental theory, such a heavy system as the Tl$^+$ ion with 80 electrons is a challenging problem for existing computational methods which can only be verified with the help of reliable measurements. Therefore, every success achieved in the field of experiment and theory is crucial for developing fundamental problems of modern physics of electron–ion collisions.
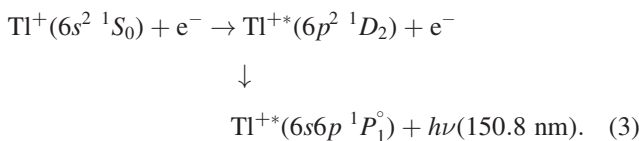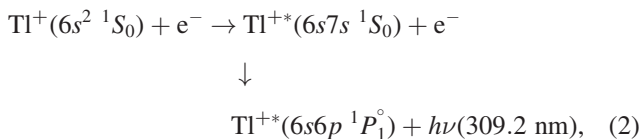
* Author to whom any correspondence should be addressed.

The Tl$^+$ ion, being isoelectronic with the Hg atom, has the $5d^{10}6s^2$ $^1S_0$ ground state electron configuration with fully filled $s$ and $d$ shells. Excitation of one $s$ electron results in the formation of a system of singlet and triplet levels of $6snl$ configurations. The simultaneous excitation of both $s$ electrons or the excitation of one $d$ electron gives rise to so-called 'shifted levels' of $5d^{10}6p^2$ and $5d^96s^26p$ configurations, respectively [4–6]. An essential feature of the arrangement of these 'shifted levels' in the Tl$^+$ ion, in comparison with the Hg atom, is that they are all located below the ionization potential of the ion. In addition, due to relativistic and correlation effects specific to heavy atomic systems [6], binding energies of $6s$ and $5d$ electrons in the Tl$^+$ ion are quite close. As a result, the role of the $5d^{10}$ shell in the excitation process significantly increases. For these reasons, transitions from the levels of $5d^{10}6p^2$ and $5d^96s^26p$ configurations to lower levels are rather effective in the Tl$^+$ ion.

Despite the significant fundamental interest and the possibility of practical applications, theoretical studies of inelastic collisions of electrons with single-charged Tl$^+$ ions are not available in the literature at present. As far as measurements are concerned, except for the experiment in [7], all others were performed in our group [8, 9].

In this paper, we present the results of experimental and theoretical studies of the effective cross section of the Tl$^+$ ion resonance line excitation by electron impact:

$$\text{Tl}^+(6s^2\ ^1S_0) + e^- \rightarrow \text{Tl}^{+*}(6s6p\ ^1P_1^\circ) + e^-$$
$$\downarrow$$
$$\text{Tl}^+(6s^2\ ^1S_0) + h\nu(132.2\ \text{nm}). \quad (1)$$

To study the contribution of cascade transitions to the cross section of the resonance transition (1), we also investigated the effective cross sections of the following spectral transitions:

$$\text{Tl}^+(6s^2\ ^1S_0) + e^- \rightarrow \text{Tl}^{+*}(6s7s\ ^1S_0) + e^-$$
$$\downarrow$$
$$\text{Tl}^{+*}(6s6p\ ^1P_1^\circ) + h\nu(309.2\ \text{nm}), \quad (2)$$

$$\text{Tl}^+(6s^2\ ^1S_0) + e^- \rightarrow \text{Tl}^{+*}(6p^2\ ^1D_2) + e^-$$
$$\downarrow$$
$$\text{Tl}^{+*}(6s6p\ ^1P_1^\circ) + h\nu(150.8\ \text{nm}). \quad (3)$$

In equations (1)–(3), Tl$^{+*}$ are the excited ionic states, $h\nu$ are the emitted photon energies.

According to the data [10], the calculated transition probabilities of these transitions, as well as the $6s6d\ ^1D_2 \rightarrow 6s6p\ ^1P_1^\circ$ (253.1 nm) transition, are shown to be the largest among all possible transitions from higher levels to the $6s6p\ ^1P_1^\circ$ level. Note that we could not measure the effective cross section of the $\lambda 253.1$ nm line excitation since this wavelength is close to the edge of the spectral range of the commercial monochromator MDR-2 used in this work. Figure 1 shows a simplified energy level diagram for the Tl$^+$ ion including the radiative transitions studied in this work.
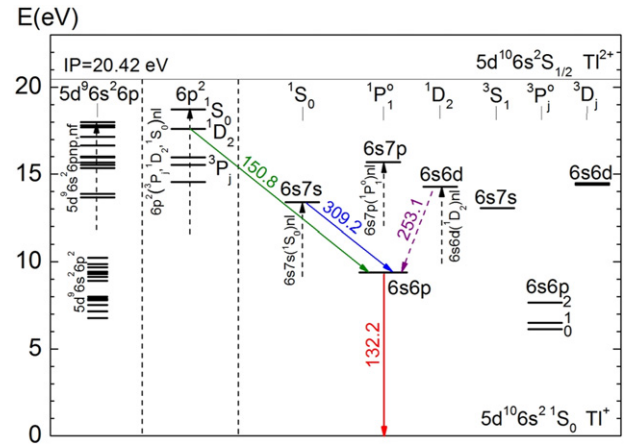


**Figure 1.** Energy level diagram for the Tl$^+$ ion.

## 2. Experiment

The experiment was performed by the spectroscopic method under the conditions of electron and ion beams intersecting at the right angle. The main components of the experimental apparatus, as well as the measurement procedure, are described in detail elsewhere [11, 12].

In an equipotential collisional region at the ambient pressure of $7 \times 10^{-6}$ Pa, a beam of Tl$^+$ ions was crossed by a beam of monoenergetic electrons (see figure 2). The ribbon electron beam with the cross sectional area of $1 \times 8$ mm$^2$ was formed by a low-energy three-electrode electron gun providing the electron current of $(10–150) \times 10^{-6}$ A with the monoenergeticity (FWHM) of 0.5–1.0 eV in the energy range of 8–300 eV. Use of the ribbon electron beam allowed us to enlarge the collision region and thereby the intensity of an emission signal. To obtain the beam of single-charged Tl$^+$ ions, the ion source operating in the mode of low-voltage arc discharge ($U < 10$ V) was used. The discharge voltage $U$ was chosen so as to prevent the formation of Tl$^+$ ions in the long-lived $6s6p\ ^3P_{0,2}^\circ$ levels ($\tau \approx 10^{-8}$ ns [13]) which could reach the interaction region and make a significant contribution to the background when measuring the excitation from the ground $5d^{10}6s^2\ ^1S_0$ level. The used ion source allowed one to obtain the collimated beam (with the cross section area of $2.5 \times 2.5$ mm$^2$) of single-charged Tl$^+$ ions mainly in the ground state with the current of $0.8 \times 10^{-6}$ A at the ion energy of 1 keV.

Emission from the interaction region resulting from the radiative transitions (equations (1)–(3)) was observed orthogonal to the ion and electron beams intersection plane. For spectral analysis of this emission, a commercial monochromator MDR-2 with a reciprocal linear dispersion of 2.0 nm mm$^{-1}$ was used in the ultraviolet (UV) and visible spectral regions, while in the vacuum ultraviolet region (VUV) this was a noncommercial VUV monochromator based on the Seya–Namioka scheme [14] with a reciprocal linear dispersion of 1.7 nm mm$^{-1}$. Commercial solar-blind FEU-142 photomultipliers were used to detect the emission signals. The spectral sensitivity of the detection system in the UV and visible spectral regions was determined from the spectral distribution
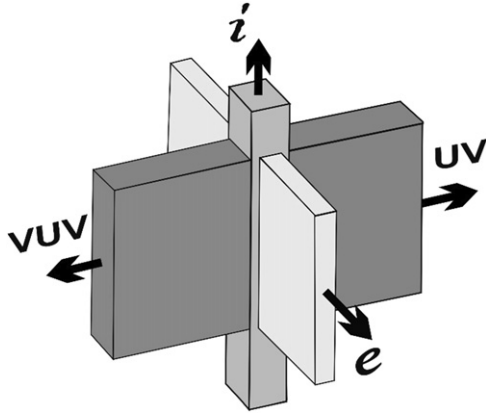
**Figure 2.** Schematic representation of the experiment (*i*—ion beam, *e*—electron beam, VUV and UV—emission from the collision region).

of the emission brightness of a commercial low-voltage arc-discharge hydrogen lamp DVS-25. In the VUV region, the spectral sensitivity was determined on the basis of the emission intensities of the atomic nitrogen spectral lines resulting from the electron impact of $N_2$ molecules measured at the electron energy of 100 eV. The calibration uncertainty of the spectral sensitivity of the detection system was about 16% in both spectral ranges.

Since the signals originating from the processes under investigation (equations (1)–(3)) were observed against a large background, arising from the interaction of both beams with the residual gas, modulation of the electron and ion beams with rectangular pulses shifted with respect to each other by a quarter of a period was used. This, in combination with a four-way chopping registration system, allows one to extract the required signal of 4–5 counts per second at the signal-to-background ratio of 0.07–0.1 for the $\lambda 132.2$ nm resonance line. In this case, the electron gun was operating in the mode providing the electron monoenergeticity of 0.5 eV. Note that in the case of the $\lambda 150.8$ nm and $\lambda 309.2$ nm lines the desired signal intensity did not exceed one count per second at the signal-to-background ratio of 0.03–0.05. In order to increase the intensity of the useful signal, relevant measurements were performed at an inferior electron monoenergeticity of 0.8–1 eV.

The uncertainty of the relative measurements did not exceed 10% in the case of the $\lambda 132.2$ nm resonance line and 30% for the $\lambda 150.8$ nm and $\lambda 309.2$ nm lines. The electron beam energy and monoenergeticity were determined with an uncertainty of no more than 0.1 eV. The excitation threshold of the $\lambda 121.6$ nm line of atomic hydrogen by electron impact was used to calibrate the electron energy scale.

## 3. Theory

Since $Tl^+$ is a heavy ion with 80 electrons, relativistic theoretical methods have to be used to study its excitation due to electron impact. In the present work, we use the relativistic distorted wave (RDW) method [15] to calculate the effective cross sections for the $6s6p$ $^1P_1^\circ \rightarrow 6s^2$ $^1S_0$ (132.2 nm),

$6s7s$ $^1S_0 \rightarrow 6s6p$ $^1P_1^\circ$ (309.2 nm), and $6p^2$ $^1D_2 \rightarrow 6s6p$ $^1P_1^\circ$ (150.8 nm) transitions. The *T*-matrix in the RDW approximation for excitation of an *N*-electron atom from its initial state *a* to the final state *b* is represented as

$$T_{a \rightarrow b}^{\text{RDW}} = \langle \chi_b^-(1, 2, \ldots, N+1) | V - U_b | A\chi_a^+(1, 2, \ldots, N+1) \rangle. \tag{4}$$

Here *V* is the interaction potential between the target atom and the projectile electron, $U_b$ refers to the distortion potential. It is chosen to be the spherically symmetric static potential of the final state of the atom so that it depends only on the projectile electron radial coordinates. *A* is the antisymmetrization operator to account for the exchange of the projectile electron with the target electrons. $\chi_{a(b)}^{+(-)}$ represents the product of the atomic wave function $\Phi_{a(b)}$ and the projectile electron distorted wave function $F_{a(b)}^{\text{DW}+(-)}$ in the initial (final) state

$$\chi_{a(b)} = \Phi_{a(b)}(1, 2, \ldots, N) F_{a(b)}^{\text{DW}+(-)}(\mathbf{k}_{a(b)}, N+1). \tag{5}$$

The atomic wave functions $\Phi_{a(b)}$ are obtained within the multiconfiguration Dirac–Fock (MCDF) [16] framework using the GRASP2K package [17]. In the MCDF approach, an atomic state function (ASF) is approximated as a linear combination of configuration state functions (CSFs) with the same parity *P* and total angular momentum quantum number *J*

$$\Phi(\gamma PJM) = \sum_{i=1}^{n} c_i \phi_i(\gamma_i PJM). \tag{6}$$

Here $c_i$ are the mixing coefficients of the CSFs $\phi_i$ which are the product of the one-electron Dirac orbitals within the active space under consideration, $\gamma_i$ are additional quantum numbers required for the unique representation of the CSFs. The expansion coefficients $c_i$ and the Dirac orbitals are optimised to self-consistency with the relativistic self-consistent field method.

In the present work, the CSFs are obtained with the multi-reference single- and double-excitation method [18] from a multi-reference set $\{5d^{10}6s^2, 5d^{10}6s6p, 5d^{10}6s7s\}$ to the active set which is systematically expanded up to $\{12s, 11p, 10d, 7f, 6g\}$ to include all possible bound states. The important core–valence correlations are considered with a maximum of two electrons allowed to be excited from the core $5d^{10}$ subshell in the defined active space. Finally, we have considered only the CSFs contributing 99.99% of a given ASF. The MCDF calculations are followed by the relativistic configuration interactions calculations to consider the Berit interaction and leading quantum electrodynamic corrections.

The distorted wave functions in equation (5) are calculated by solving the coupled Dirac equations using the distortion potential $U_b$. The details can be found in our previous work [15], where the notation $V_d$ was used in place of the $U_b$. Thus, after obtaining the atomic and projectile electron wave functions, the *T*-matrix (equation (4)) can be computed. Finally,

the electron impact excitation cross section is calculated as

$$\sigma_{a\to b} = (2\pi)^4 \frac{k_b}{2(2J_a+1)k_a} \sum_{M_a\mu_a M_b\mu_b}$$
$$\int |T_{a\to b}^{\mathrm{RDW}}(\gamma_b, J_b, M_b, \mu_b; \gamma_a, J_a, M_a, \mu_a)|^2 \mathrm{d}\Omega. \quad (7)$$

Here $J_{a(b)}$ represents the total angular momentum quantum number of the initial (final) state, $M_{a(b)}$ is the corresponding magnetic quantum number, $k_{a(b)}$ denotes the projectile electron wave vector in the initial (final) channel, and $\mu_{a(b)}$ is the spin projection of the incident (scattered) electron.

To obtain the effective cross sections, we take into account two possible ways to populate a level. The first one is due to direct electron impact excitation from the ground state to all possible excited bound states which can further decay radiatively to the level of interest, namely $6s6p\ ^1P_1^\circ$ or $6s7s\ ^1S_0$ or $6p^2\ ^1D_2$. In the present work, we considered a total of 100 excited levels of $\mathrm{Tl}^+$. The second way is to take into account direct excitation of $6s7s\ ^1S_0$ or $6p^2\ ^1D_2$ state from the excited $6s6p\ ^3P_{0,1,2}^\circ$, $^1P_1^\circ$ states, in addition to the ground state. Since there are more than one radiative decay channel of the excited states to the lower level of interest, we obtained the branching fractions for each such channel. The excitation cross sections from the ground state to the higher levels are multiplied by their corresponding branching fractions and added to the direct excitation cross sections from the ground and the excited states. These summed up cross sections give directly the effective cross section for the resonance $6s6p\ ^1P_1^\circ \to 6s^2\ ^1S_0$ transition. However, for the $6s7s\ ^1S_0$ and $6p^2\ ^1D_2$ levels, more than one decay channel is present. The branching fractions are 0.87 and 0.40 for the $6s7s\ ^1S_0 \to 6s6p\ ^1P_1^\circ$ and $6p^2\ ^1D_2 \to 6s6p\ ^1P_1^\circ$ transitions, respectively. The summed up cross sections for these levels are multiplied by the respective branching fractions of the transitions to obtain the effective cross sections.

## 4. Results and discussion

The electron impact effective cross sections are studied in the energy range from the excitation thresholds up to 300 eV for the resonance $6s6p\ ^1P_1^\circ \to 6s^2\ ^1S_0$ (132.2 nm) transition and up to 100 eV for the $6s7s\ ^1S_0 \to 6s6p\ ^1P_1^\circ$ (309.2 nm) and $6p^2\ ^1D_2 \to 6s6p\ ^1P_1^\circ$ (150.8 nm) cascade transitions. The results of the measurements together with the theoretical calculations are presented in figure 3.

As can be seen, the experimentally-measured effective cross section in the case of the resonance $6s6p\ ^1P_1^\circ \to 6s^2\ ^1S_0$ (132.2 nm) transition rapidly increases at the threshold ($E_{\mathrm{th}} \approx 9.4$ eV) and has a pronounced structure in a wide range of electron energies. The observed structure arises from the population of the resonance $6s6p\ ^1P_1^\circ$ level due to the resonance effects resulting from the formation and electron decay of autoionizing states (AIS) of the Tl atom, as well as radiative cascade transitions from higher levels of the $\mathrm{Tl}^+$ ion. Above 70 eV, the cross section falls according to the $E^{-1}\ln E$ law which is characteristic of optically allowed transitions.
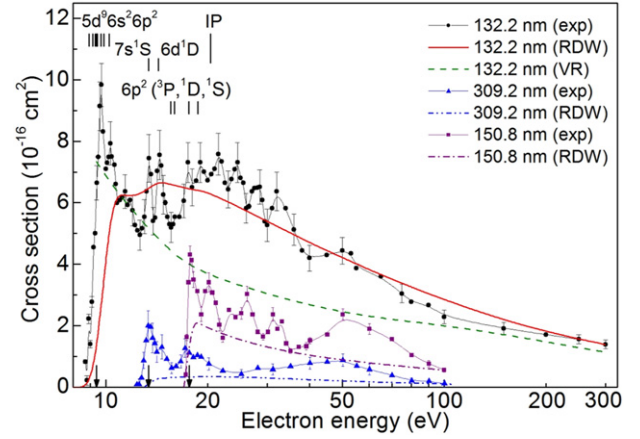


**Figure 3.** Absolute effective cross sections for the $\lambda 132.2$ nm ($6s6p\ ^1P_1^\circ \to 6s^2\ ^1S$), $\lambda 309.2$ nm ($6s7s\ ^1S_0 \to 6s6p\ ^1P_1^\circ$), and $\lambda 150.8$ nm ($6p^2\ ^1D_2 \to 6s6p\ ^1P_1^\circ$) lines (exp—experiment, RDW—calculation using the RDW approximation, VR—calculation using the Van Regemorter formula [26], IP—$\mathrm{Tl}^+$ ionization potential, vertical arrows—line excitation thresholds).

In the near-threshold energy range, below the energy of the first excited $6s7s\ ^3S_1$ level ($\approx 13$ eV) from which the transition to the $6s6p\ ^1P_1^\circ$ level is already possible, the structure can be explained only by the resonance contribution of the AIS. In particular, two features at 9.7 eV and 10.3 eV result from the decay of the atomic AIS of the $5d^9 6s^2 6p^2$ configuration lying in the energy range 9.1–10.2 eV [19–22].

The structure observed in the energy range from 13 eV up to the $\mathrm{Tl}^+$ ionization potential (20.4 eV) is mainly due to the cascade transitions from higher ionic levels. Thus, two pronounced features at 13.4 eV and 14.4 eV are related to the transitions from the $6s7s\ ^1S_0$ and $6s6d\ ^1D_2$ ionic levels. In the case of the maximum at 13.4 eV, this is confirmed by a good correlation between this maximum and the maximum in the threshold range of the effective cross section for the $6s7s\ ^1S_0 \to 6s6p\ ^1P_1^\circ$ cascade transition (see the 309.2 nm (exp) curve in figure 3). In addition, the atomic AIS of the $5d^{10}6s7s(^1S)np$ ($n \geqslant 7$), $5d^{10}6s6d(^1D)np$ ($n \geqslant 8$), and $5d^{10}6s6d(^1D)nd$ ($n \geqslant 6$) configurations [22] converging to the $6s7s\ ^1S_0$ and $6s6d\ ^1D_2$ ionic levels also contribute to the above maxima at 13.4 eV and 14.4 eV.

According to the data [4–6], the $6p^2\ ^3P_{0,1,2}$, $^1D_2$, and $^1S_0$ levels fall within the energy range of 14.6–18.7 eV. The structure observed in the effective cross section of the resonance line (132.2 nm) at 17.5 eV and 18.9 eV results from the cascade contribution of the $6p^2\ ^1D_2$ (see the $\lambda 150.8$ nm (exp) curve in figures 3) and $6p^2\ ^1S_0$ ionic levels as well as the atomic AIS converging to them. As for the $6p^2\ ^3P_{0,1,2}$ levels (14.6–16.0 eV), there is a rather deep minimum in the cross section in the vicinity of 15.3 eV. This, in our opinion, is indicative of the low probability of the transitions from these levels to the $6s6p\ ^1P_1^\circ$ level.

It is worth noting that in the energy range 13.7–18 eV ionic levels of the $5d^9 6s^2 6p$ configuration [4, 5, 19, 21, 23] can also play a role in the population of the resonance $6s6p\ ^1P_1^\circ$ level. Direct transitions from these levels to the resonance $6s6p\ ^1P_1^\circ$ level are forbidden by the parity selection rules. However,

these levels can contribute to the resonance level population due to the cascade transitions via lower even-parity excited ionic levels, particularly the $6s7s$ $^1S_0$ and $6s6d$ $^1D_2$ levels. In addition, each of the ionic $5d^96s^26p$ levels is the convergence limit of the atomic AIS of the $5d^96s^26pnp$ ($n \geqslant 7$) and $5d^96s^26pmf$ ($m \geqslant 5$) configurations [22]. These AIS also make a resonance contribution to the lines under study, both directly and via cascades.

The structure observed in the energy range above the Tl$^+$ ionization potential (20.4 eV) is the result of two main processes: (i) excitation of an electron of the $5d^{10}$ shell with the formation of the ionic AIS of the $5d^96s^2np$ and $5d^96s^2nd$ ($n \geqslant 6$) configurations and (ii) simultaneous excitation of two electrons of the $5d^{10}$ and $6s^2$ shells resulting in the formation of the ionic AIS of the $5d^96s6p^2$ configuration. Note that there are no data on such states for the Tl$^+$ ion available in the literature. However, data on such states can be found for other ions of group III, e.g. the In$^+$ ion [24, 25]. According to the selection rules, the AIS of the $5d^96s6p^2$ configuration can radiatively decay to the resonance $6s6p$ $^1P_1^\circ$ level making an additional contribution to its population. The same processes are responsible for the structure observed in the cross section of the $\lambda150.8$ nm line above 20.4 eV. The features in the effective excitation cross sections for the $\lambda150.8$ nm and $\lambda132.2$ nm lines show a noticeable correlation in the structure. This indicates that the cascade contribution from the $6p^2$ $^1D_2$ level to the resonance $6s6p$ $^1P_1^\circ$ level occurs in a wide energy range.

The broad maximum near about 50 eV observed in the effective cross sections of all three lines is most likely related to *d*-shell ionization with or without the excitation of an electron of the valence $6s^2$ shell of the Tl$^+$ ion.

The absolute values of the effective excitation cross section for the resonance $6s6p$ $^1P_1^\circ \rightarrow 6s^2$ $^1S_0$ (132.2 nm) as well as cascade $6s7s$ $^1S_0 \rightarrow 6s6p$ $^1P_1^\circ$ (309.2 nm) and $6p^2$ $^1D_2 \rightarrow 6s6p$ $^1P_1^\circ$ (150.8 nm) transitions are obtained by normalizing the experimental data using the RDW cross sections. The first cross section is normalized at 300 eV while the latter two are normalized at 100 eV incident electron energy. The corresponding cross sections are found to be $1.39 \times 10^{-16}$ cm$^2$ (132.2 nm), $0.11 \times 10^{-16}$ cm$^2$ (309.2 nm), and $0.56 \times 10^{-16}$ cm$^2$ (150.8 nm). The calculated effective cross sections for the transitions at 132.2 nm and 150.8 nm show an overall good agreement with the measurements. In the case of the 309.2 nm line, the RDW calculation gives a smaller value of the cross section than the normalized measurement. Since we did not include other inelastic channels such as autoionization, electron attachment, etc in the RDW calculations, the structures are missing in the theoretical cross sections. Furthermore, the present calculations are performed in the first order RDW approximation. These results are expected to be more reliable from intermediate to high energies.

For comparison, the absolute effective excitation cross section of the resonance $\lambda132.2$ nm line calculated using the semi-empirical Van Regemorter formula [26] is also presented in figure 3 (see 132.2 nm (VR) curve). As can be seen, at high energies (200–300 eV) the cross section in this case is in good agreement with that calculated using the

RDW approximation. At lower energies a considerable discrepancy with both the RDW calculation and the experiment is observed.

## 5. Conclusions

The electron-impact excitation of the resonance $6s6p$ $^1P_1^\circ \rightarrow 6s^2$ $^1S_0$ (132.2 nm), as well as the cascade $6s7s$ $^1S_0 \rightarrow 6s6p$ $^1P_1^\circ$ (309.2 nm) and $6p^2$ $^1D_2 \rightarrow 6s6p$ $^1P_1^\circ$ (150.8 nm) spectral transitions from the ground $6s^2$ $^1S_0$ level in the Tl$^+$ ion, is studied. The distinct structure observed in the cross section of the $\lambda132.2$ nm resonance line in the energy range below the Tl$^+$ ionization potential (20.4 eV) results mainly from the population of the $6s6p$ $^1P_1^\circ$ level. This is due to the resonance capture of an incident electron giving rise to the formation and subsequent electron decay of the AIS of the Tl atom of $5d^96s^26p^2$, $5d^{10}6s7s(^1S)np$ ($n \geqslant 7$), $5d^{10}6s6d(^1D)np$ ($n \geqslant 6$), and $5d^{10}6s6d(^1D)nd$ ($n \geqslant 6$) configurations, as well as radiative transitions from the higher $6s7s$ $^1S_0$, $6s6d$ $^1D_2$, and $6p^2$ $^1D_2$, $^1S_0$ levels of the Tl$^+$ ion. Above the ionization potential, two main processes are responsible for the observed structure. These are (i) the excitation of one of the $5d^{10}$ shell electrons and (ii) the simultaneous excitation of two electrons of the $5d^{10}$ and $6s^2$ shells leading to the formation of ionic AIS of the $5d^96s^2np$, $5d^96s^2nd$, and $5d^96snp$ ($n \geqslant 6$) configurations. Their radiative decay to the resonance $6s6p$ $^1P_1^\circ$ level makes an additional contribution to its population. The broad maximum close to 50 eV observed in the effective cross sections of all lines under study is most likely due to $5d$ shell ionization, which may or may not be accompanied by the excitation of the $6s^2$ valence shell electron. The correlation between the cross section structures of the resonance $6s6p$ $^1P_1^\circ \rightarrow 6s^2$ $^1S_0$ (132.2 nm) and cascade $6p^2$ $^1D_2 \rightarrow 6s6p$ $^1P_1^\circ$ (150.8 nm) transitions indicates that the cascade contribution from the $6p^2$ $^1D_2$ level to the resonance $6s6p$ $^1P_1^\circ$ level occurs in the wide energy range.

We carried out the RDW calculations to study the three transitions mentioned above. The agreement between the measurements and the RDW calculations is rather good for the $\lambda132.2$ nm and $\lambda150.8$ nm lines, while in the case of the $\lambda309.2$ nm line the theoretical cross section is smaller than the measured one. The inclusion of more inelastic channels may be necessary to study cascade effects and improve the agreement between the theory and the experiment.

The absolute values of the effective excitation cross section are found to be $1.39 \times 10^{-16}$ cm$^2$ at the incident electron energy of 300 eV for the resonance $6s6p$ $^1P_1^\circ \rightarrow 6s^2$ $^1S_0$ (132.2 nm) transition, $0.11 \times 10^{-16}$ cm$^2$ and $0.56 \times 10^{-16}$ cm$^2$ at the incident electron energy of 100 eV for the cascade $6s7s$ $^1S_0 \rightarrow 6s6p$ $^1P_1^\circ$ (309.2 nm) and $6p^2$ $^1D_2 \rightarrow 6s6p$ $^1P_1^\circ$ (150.8 nm) transitions, respectively. The absolute cross section values for all three transitions are obtained by normalizing the experimental data to those calculated using the RDW approximation. The obtained values indicate that the contribution of the cascade transitions under study to the effective cross section of the $\lambda132.2$ nm resonance line at the energy of 100 eV is about 30%.

A calculation using the semi-empirical Van Regemorter formula is also performed to obtain the effective cross section of the resonance $\lambda 132.2$ nm line. The absolute value of the cross section at high energies (200–300 eV) is found to be nearly the same as given by the RDW calculation, while at lower energies a considerable discrepancy with both the RDW calculation and the experiment is observed.

## Data availability statement

The data that support the findings of this study are available upon reasonable request from the authors.

## ORCID iDs

Viktoria Roman ⓘ https://orcid.org/0000-0003-2499-8357
Aleksandr I Gomonai ⓘ https://orcid.org/0000-0003-4341-699X
Lalita Sharma ⓘ https://orcid.org/0000-0003-0316-0977
Aloka Kumar Sahoo ⓘ https://orcid.org/0000-0003-2441-4075
Anna N Gomonai ⓘ https://orcid.org/0000-0003-3304-0773

## References

[1] Shimizu A, Fujisawa A, Ohshima S, Nakano H, Minami T, Isobe M, Okamura S and Matsuoka K 2018 *Rev. Sci. Instrum.* **89** 113507
[2] Leckrone D S, Johansson S, Kalus G, Wahlgren G M, Brage T and Proffitt C R 1996 *Astrophys. J.* **462** 937
[3] Johansson S, Kalus G, Brage T, Leckrone D S and Wahlgren G M 1996 *Astrophys. J.* **462** 943
[4] Moore C E 1971 *Atomic Energy Levels as Derived from Analyses of Optical Spectra* (Washington, DC, USA: National Bureau of Standards) p 245
[5] Kramida A, Yu R, Reader J and NIST ASD Team 2021 *NIST Atomic Spectra Database (version 5.9)* (Gaithersburg, MD, USA: National Institute of Standards and Technology) https://doi.org/10.18434/T4W30F
[6] Wilson M 1985 *Phys. Lett.* A **111** 363
[7] Divine T F, Feeney R K, Sayle W E and Hooper J W 1976 *Phys. Rev.* A **13** 54
[8] Zapesochnyi I P, Imre A I, Kontrosh E E, Zapesochnyi A I and Gomonai A N 1986 *JETP Lett.* **43** 596
[9] Gomonai A N, Imre A I and Kontrosh E E 1996 *Opt Spectrosc.* **81** 22
[10] de Andrés-García I, Colón C and Fernández-Martínez F 2018 *Mon. Not. R. Astron. Soc.* **476** 793
[11] Gomonai A N, Imre A I and Vukstich V S 2005 *Opt. Spectrosc.* **99** 849
[12] Ovcharenko E V, Imre A I, Gomonai A N and Hutych Y I 2010 *J. Phys. B: At. Mol. Opt. Phys.* **43** 175206
[13] Henderson M and Curtis L J 1996 *J. Phys. B: At. Mol. Opt. Phys.* **29** L629
[14] Maletta A M and Johnson P M 2000 *Rev. Sci. Instrum.* **71** 3653
[15] Sharma L, Surzhykov A, Srivastava R and Fritzsche S 2011 *Phys. Rev.* A **83** 062701
[16] Grant I P 2007 *Relativistic Quantum Theory of Atoms and Molecules* (New York: Springer)
[17] Jönsson P, Gaigalas G, Bieroń J, Froese Fischer C and Grant I P 2013 *Comput. Phys. Commun.* **184** 2197
[18] Fischer C F, Godefroid M, Brage T, Jönsson P and Gaigalas G 2016 *J. Phys. B: At. Mol. Opt. Phys.* **49** 182004
[19] Connerade J P 1972 *Astrophys. J.* **172** 213
[20] Connerade J P, Garton W R S, Mansfield M W D and Martin M A P 1976 *Proc. R. Soc.* A **350** 47
[21] Connerade J P 1979 *J. Phys. B: At. Mol. Phys.* **12** L223
[22] Back C, Pejcev V, Ross K J and Wilson M 1983 *J. Phys. B: At. Mol. Phys.* **16** 2413
[23] Martin W, Sugar J and Tech J L 1972 *Phys. Rev.* A **6** 2022
[24] Duffy G and Dunne P 2001 *J. Phys. B: At. Mol. Opt. Phys.* **34** L173
[25] Kilbane D, Mosnier J-P, Kennedy E T, Costello J T and van Kampen P 2006 *J. Phys. B: At. Mol. Opt. Phys.* **39** 773
[26] Sobel'man I I, Vainshtein L A and Yukov E A 1995 *Excitation of Atoms and Broadening of Spectral Lines* (Berlin: Springer)